24th International Conference on Renewable Energies and Power Quality (ICREPQ'26)
Santander (Spain), 10th to 12th June 2026
E&Q Journal - ISSN:2659-8779. Volume 4. July 2026

Performance Analysis of Segregated Phase Comparison Line Differential Protection in Networks with Inverter-Based Resources

B. Agudelo-Cruz, M. Alzate-Posso and J. Mora-Flórez

ICE[3] Research Group, Electrical Engineering Program
Universidad Tecnológica de Pereira
Campus La Julita, 660003, Pereira, Colombia. colxiver.agudelo, marcos.alzate, jjmora@utp.edu.co

Abstract

Electric power systems with high penetration of inverter-based distributed generation face significant technical and operational challenges, among which protection systems constitute a critical concern. This paper presents a comparative assessment of a conventional segregated phase comparison–based line differential protection scheme and a proposed approach that incorporates compensation for line capacitance effects in networks with inverter-based resources (IBRs). For this purpose, a detailed electromagnetic transient model of the test system was developed in PSCAD/EMTDC. Various fault scenarios, including single-phase-to-ground, phase-to-phase, and three-phase-to-ground faults, were simulated under different fault resistance conditions. In addition, the influence of variations in sampling frequency on the performance of both protection schemes was investigated.

Simulation results demonstrate that the proposed secure segregated phase comparison–based differential protection scheme effectively mitigates angular difference oscillations and maintains a nearly constant response under pre-fault steady-state conditions. These characteristics significantly enhance the reliability, selectivity, and operating speed of line protection, particularly in converter-dominated power feeders.

Key words: Inverter-based resources, line protection, distributed energy resources, and phase comparison.

1. Introduction

1.1 Motivation

Currently, power systems worldwide face new operational challenges due to the increasing integration of inverter-based resources (IBRs). In countries with high levels of renewable generation penetration, critical events and disturbances have been reported in power networks, highlighting the need to reassess and adapt traditional system planning, operation, and protection strategies [1].

This situation is largely attributable to the predominance of IBRs, particularly grid-following units, which rely on the power system to establish their voltage and frequency references. Under fault or disturbance conditions, these IBRs may adversely affect system efficiency because they attempt to resynchronise via their internal phase-locked loop (PLL). This process can lead to undesirable oscillations and impede the restoration of synchronism, thereby directly affecting the system's rapid recovery [1], [2].

Consequently, the integration of IBRs impacts the performance and reliability of conventional protection schemes. Furthermore, the IBRs fault behaviour, influenced by internal control mechanisms, complicates the detection and coordination of protection systems originally designed for networks dominated by synchronous generators. This may result in protective relays failing to operate correctly during fault conditions or operating inappropriately, thereby compromising the sensitivity and stability of protection systems [3]. Line differential protection also faces challenges in conventional power networks, including synchronisation issues, cybersecurity concerns, capacitive effects, loading conditions, weak-infeed conditions, and power-line-related issues [4].

1.2 State of Art

Mainly, grid-following inverters rely on the power network to establish voltage and frequency references through phase-locked loops (PLLs). During disturbances and fault conditions, this characteristic may induce oscillations and grid control interaction phenomena that degrade system stability and alter the electrical quantities measured by protection devices. Consequently, conventional relays may experience coordination failures, unwanted tripping, or insensitivity to internal faults, due to the limited fault current contribution of IBRs and the harmonic distortions associated with converter control [4].

Several adaptive protection strategies have been developed for overcurrent, distance, and differential schemes. Optimisation-based approaches have been used to adjust pickup currents and coordination times in order to preserve selectivity under variations of the IBRs fault current contribution for directional overcurrent protection [5]. However, distance protection may be limited in weak infeed scenarios, for example, when a line connects a strong source at one end and a weak or renewable-based source at the other. Under such conditions, the apparent impedance may shift and fall outside the predefined operating zones [6].

Given the limitations of overcurrent and distance-based approaches, line differential protection stands out by comparing currents at both terminals, providing reliability for internal and external faults. Nevertheless, in systems with IBDERs, its reliability may be degraded by disturbances in unfaulted phases and by the low-impedance zero-sequence paths in transformers. These effects impair phase discrimination and compromise the stability of the operating characteristic [7]. Among the advances aimed at strengthening the differential criterion, phase-comparison techniques have been reported [8]. For example, a current mapping strategy is used to redefine differential and restraint currents by transforming these measurements at both line terminals. This complex-domain representation can produce more stable trajectories and improve sensitivity and separation between internal and external faults in the presence of IBRs [9]. Additionally, current transformer saturation remains a critical challenge; fast saturation detection algorithms have been proposed to dynamically adjust sensitivity under external fault conditions, thereby mitigating spurious operations during the initial stages of the event [10]. Recent literature has also explored next-generation approaches, such as setting-less protection, which relies on dynamic state estimation and statistical testing to verify, in real time, the consistency between measurements and physical component models. These strategies aim to reduce dependence on fixed parameter settings and to enhance performance under varying operating conditions, including networks with high converter penetration [11]. Finally, several adaptive approaches have been proposed for differential protection, as presented in [12]; these algorithms adjust the protection zones based on the current state of the power system.

1.3 Contributions

The most important contributions of this paper are: a) Analysis of the performance of non-adaptive and adaptive α-plane based line differential protection in IBR polluted power systems; and b) Determination of the influence of the type of fault, sampling frequency, fault location, and fault resistance on the performance of the differential protection.

2. Segregated phase comparison based line differential protection

Phase comparison evaluates the angular phase shift between line currents measured at both terminals [13]. Secure operation requires a reliable communication channel between relays, with appropriate compensation for channel latency to ensure temporal coherence between the signals being compared.

2.1 Conventional segregated phase comparison technique

This technique uses the phase currents at nodes i and j of the transmission line, along with the residual current associated with the zero-sequence component. The phase angle difference is calculated as shown in equation (1).

$$\begin{bmatrix}\psi_a\\ \psi_b\\ \psi_c\\ \psi_0\end{bmatrix} = \begin{bmatrix}\angle I_{ij}^{line}(a)\\ \angle I_{ij}^{line}(b)\\ \angle I_{ij}^{line}(c)\\ \angle I_{ij0}^{line}\end{bmatrix} - \begin{bmatrix}\angle I_{ji}^{line}(a)\\ \angle I_{ji}^{line}(b)\\ \angle I_{ji}^{line}(c)\\ \angle I_{ji0}^{line}\end{bmatrix} \tag{1}$$

The segregated phase comparison exhibits, in the absence of an internal fault, an angular difference between the currents measured at both terminals of 180°, due to the opposite direction of the load currents. However, this ideal value is affected by the phase shift introduced by the line capacitive charging currents, which is represented by an angular error term or compensation angle θ_c. In modern differential relays, this effect must be considered, since the associated compensation increases the effective stability angle, or restraining angle Θ_s, particularly in long transmission lines or during external faults [14]. Thus, the non-operation condition can be expressed as indicated in equation (2) [8].

$$\psi_k \in [180^\circ - (\Theta_c + \Theta_s),\ 180^\circ + (\Theta_c + \Theta_s)]\quad k \in \{a,b,c,0\} \tag{2}$$

When the angular difference ψ_k of one or more phases lies outside this restraining region, the phase comparison criterion indicates the presence of an internal fault. In practice, a decision logic is used that requires that at least two of the four angular comparisons (phases a, b, c, and residual component) indicate a fault condition, in order to increase the security of the scheme against external disturbances and measurement errors.

2.2 Secure segregated phase comparison technique

One of the main limitations of conventional segregated phase comparison schemes is the influence of line charging currents associated with the shunt capacitance, which introduce an angular error θ_c and effectively enlarge the restraining region. Although this effect can be compensated by estimating θ_c from the ratio between the charging current and the modulating quantity, its practical implementation is complex, as it requires knowing the charging current I_c. To overcome this limitation, the elimination of the angular error θ_c is achieved using the line parameters [8]. This approach relies on the three-phase π-equivalent line model, together with the line currents I_{ij}^{line} and I_{ji}^{line} measured by the CTs and the nodal voltages V_i and V_j measured by the PTs, enabling an analytical separation of the contribution associated with the shunt capacitance.

Equations (3) and (4) presents the line currents measured in each phase (a,b,c) as a function of the line parameters for nodes i and j. These expressions can be rearranged to obtain the currents associated with the series impedance of the π model defined as I_{ij}^{ser} and I_{ji}^{ser}.

$$\begin{bmatrix} I_{ij}^{line}(a) \\ I_{ij}^{line}(b) \\ I_{ij}^{line}(c) \end{bmatrix} = \begin{bmatrix} I_{ij}^{ser}(a) \\ I_{ij}^{ser}(b) \\ I_{ij}^{ser}(c) \end{bmatrix} + \frac{j}{2} \begin{bmatrix} B_{aa} & B_{ab} & B_{ac} \\ B_{ba} & B_{bb} & B_{bc} \\ B_{ca} & B_{cb} & B_{cc} \end{bmatrix} \begin{bmatrix} V_i(a) \\ V_i(b) \\ V_i(c) \end{bmatrix} \quad (3)$$

$$\begin{bmatrix} I_{ji}^{line}(a) \\ I_{ji}^{line}(b) \\ I_{ji}^{line}(c) \end{bmatrix} = \begin{bmatrix} I_{ji}^{ser}(a) \\ I_{ji}^{ser}(b) \\ I_{ji}^{ser}(c) \end{bmatrix} + \frac{j}{2} \begin{bmatrix} B_{aa} & B_{ab} & B_{ac} \\ B_{ba} & B_{bb} & B_{bc} \\ B_{ca} & B_{cb} & B_{cc} \end{bmatrix} \begin{bmatrix} V_j(a) \\ V_j(b) \\ V_j(c) \end{bmatrix} \quad (4)$$

As modern digital relays enable synchronized voltage and current phasors from sampled signals, the angle difference can be computed as shown in equation (5).

$$\Psi^{\text{ser}} = \begin{bmatrix} \angle I_{ij}^{\text{ser}}(a) - \angle I_{ji}^{\text{ser}}(a) \\ \angle I_{ij}^{\text{ser}}(b) - \angle I_{ji}^{\text{ser}}(b) \\ \angle I_{ij}^{\text{ser}}(c) - \angle I_{ji}^{\text{ser}}(c) \end{bmatrix} \quad (5)$$

Under normal operating conditions or during external faults, the series currents flowing through the line impedance at both terminals have equal magnitudes and are in phase opposition. Consequently, the decision criterion relies exclusively on comparing the phase angles of the estimated series currents (Ψ^{ser}), which ideally corresponds to an angular separation of 180°.

In the case of an external fault, it is assumed that the fault point is located at a distance A from bus i. Under this condition, the fault current corresponding to phase a can be expressed in terms of the currents associated with the series branch of the line, as shown in equation (6).

$$I_f(a) = I_{ij}^{\text{ser}}(a) + I_{ji}^{\text{ser}}(a) \quad (6)$$

From this definition, the series current in the $i \to j$ direction can be represented as a function of the fault current as

$$I_{ij}^{\text{ser}}(a) = \frac{I_f(a)\,(1-A)\,Z_s}{Z_s} \quad (7)$$

The expression (7) allows describing current $I_{ij}^{\text{ser}}(a)$ directly as a function of the fault current. Substituting equation (6) into (7).

$$I_{ij}^{\text{ser}}(a) = \frac{1-A}{A}\, I_{ji}^{\text{ser}}(a) \quad (8)$$

Thus, the angular ratio no longer equals -1. Consequently, the absolute value of the angle of the quotient between the series currents (Ψ^{ser}) no longer corresponds to 180°.

By explicitly including the shunt capacitance of the line in the model, the angular error associated with the capacitive effect is inherently accounted for, making it unnecessary to introduce the compensation angle θ_c. Under this assumption, the non-operation condition of the phase comparison scheme is defined as in equation (9).

$$\psi_k \in [180^\circ - \Theta_s,\ 180^\circ + \Theta_s], \qquad k \in \{a,b,c,0\} \quad (9)$$

This condition establishes the restraining region of the scheme and defines the operating and blocking zones of the phase comparison protection, without explicitly considering the angle θ_c.

3. Tests and results

This section presents an analysis of the results of testing segregated-phase comparison line-based differential protection under various fault scenarios along the transmission line. The analysis focuses on the ability of two strategies to discriminate among pre-fault conditions, internal faults, and external faults using the behaviour of measurements at the local and remote line ends.

3.1 Test system

Fig. 1 depicts the test system used to validate the proposed differential protection. This power network includes a grid following the IBR, which supplies 60 [MVA] at 66 [kV] line voltage at the POI to a conventional power network via line L_1. This power system is modelled using PSCAD. The line L_1 is protected using differential protection.

3.2 Testing scenarios and relay adjustments

The faults considered are single-phase-to-ground, phase-to-phase, and three-phase-to-ground faults. Additionally, fault resistances of $R_f = 0\ \Omega$ and $R_f = 10\ \Omega$ are considered, as well as sampling resolutions of 16 and 1024 samples per cycle. In this paper, the definition of the restraining angle θ_s is based on the proposal in [15], which corresponds to $\theta_s = \pm 0.9^\circ$. However, in order to strengthen the analysis and verify whether such a restraint is viable, the method was initially implemented without compensation for the line capacitive effect; that is, the steady-state pre-fault angular difference was calculated using only the currents at the two line ends (I_{ij} and I_{ji}). Additionally, the average value of the steady-state pre-fault angular difference without capacitive compensation is approximately 180.91°, corresponding to a deviation of 0.91° with respect to the ideal value of 180° under stable pre-fault conditions. In this case, if capacitive compensation were not performed, it would be necessary to consider an additional error angle, θ_c, above the value proposed in [15], due to the increase of the restraining zone. However, by calculating the currents using the voltages and the line parameters, the steady-state pre-fault angular difference is 179.99°. This value lies within the margin established in [15], which validates the appropriate selection of the restraining angle θ_s for the analysed protection scheme. Finally, for comparison, a persistence counter value of $k = 8$ is used to determine the fault state in both protection approaches.

3.3 Testing results and analysis

In this section, the results obtained for the algorithm based on the secure segregated phase comparison technique and its phasorial-domain version with capacitive compensation are presented, accounting for variations in the main system parameters. The effect of the fault resistance ($R_f = 0$ and $10\ \Omega$) is analysed for a location of 50% of the line with 1024 and 16 samples per cycle. Finally, the relay's performance under external faults is analysed.

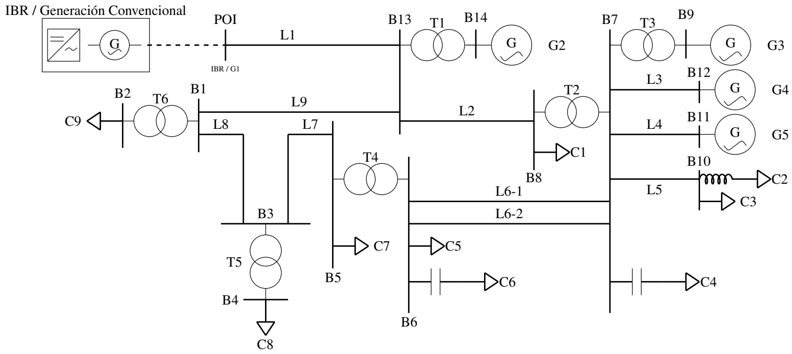

Figure 1: Single-line diagram of the test system with IBR and conventional generation.

3.3.1 Performance for fault resistance variation

According to the results depicted in Figures 2 and 3, for a single-phase-to ground fault on phase A at 2 s and a three-phase fault, considering 0 and 10 Ω values of fault resistance, and a fault trip considering 8 signal samples outside the restrain zone ($k = 8$), and a sampling frequency of 1024 samples per cycle, both the conventional (Conv) and the secure (Secure) segregated phase comparison based differential line protection, performs adequately after the fault inception (2 s). Relay trips in all cases in $t_{\text{trip}} \leq 1.25$ s.

Additionally, the secure segregated phase comparison reduces the steady-state pre-fault angle error associated with line capacitance. On the other hand, the conventional approach experiences values of ψ outside the restrain zone before the fault inception, representing a potential problem of this technique, as it sends a trip in the case of angles (ψ_A, ψ_B, ψ_C, or ψ_0) leaves the restrain zone. Finally, the analysis considers two fault-resistance values for single-phase-to-ground and three-phase-to-ground faults, as the relay behaves similarly for double-phase faults.

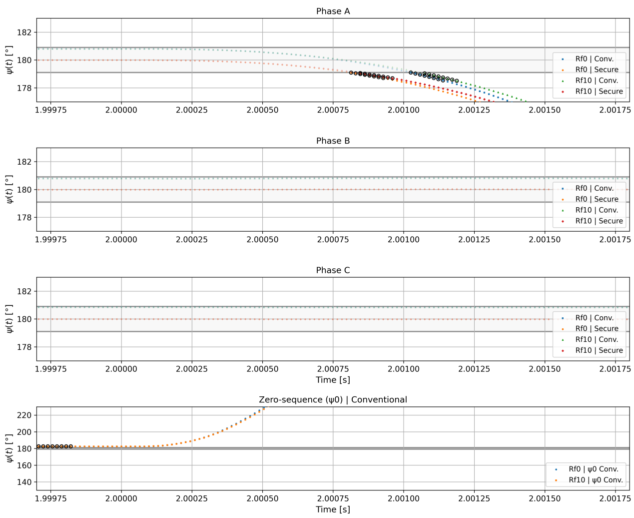

Figure 2: Protection performance for a single phase to ground fault located at 50 % of the line, considering fault resistances $R_f = 0$ Ω and $R_f = 10$ Ω, using 1024 samples per cycle.

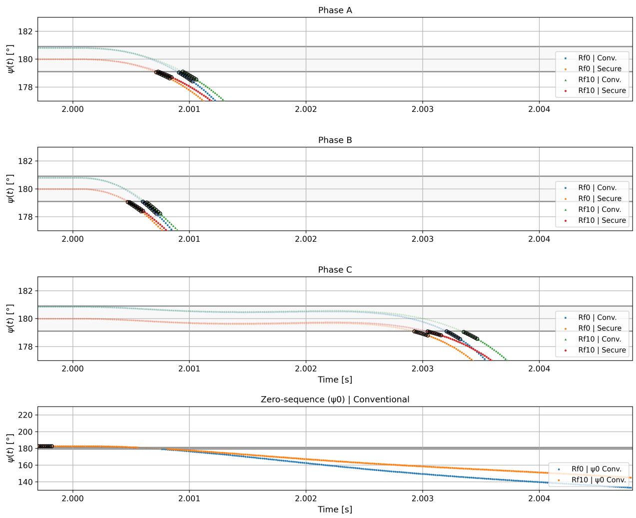

Figure 3: Protection performance for a three-phase-to-ground fault located at 50 % of the line, considering fault resistances $R_f = 0$ Ω and $R_f = 10$ Ω, using 1024 samples per cycle.

3.3.2 Performance for sampling frequency variation

Figure 4 and shows the behaviour of the conventional and secure phase comparison-based differential line protection for a sampling frequency of 16 samples per cycle, and for a single-phase fault at situations analysed in section 3.3.1. Despite the reduced number of samples, the differential protection approaches maintain a performance for the analysed fault types, similar to the previous cases. However, an inadequate performance is presented in the case of 10 Ω fault resistance, which leaves the restrained zone after a fault in phase A. Additionally, the zero-sequence component (ψ_0) of the conventional approach is outside the restraint threshold before the fault, representing a problem.

In the conventional algorithm, all phases exhibit, under steady-state conditions, an angular difference close to the restraining limit ($180° \pm 0.9°$). Under this condition, when a reduced resolution of 16 samples per cycle is employed, estimation errors associated with the transient interval between the pre-fault and fault states cause some samples to be evaluated outside the restraining region. As a result, phase C leaves the permitted band earlier than in the case of 1024 samples per cycle, highlighting the sensitivity of the

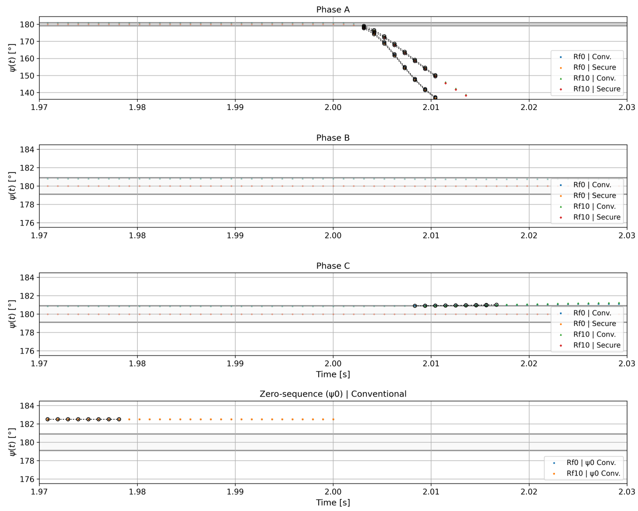

Figure 4: Protection performance for a single-phase-to-ground fault located at 50 % of the line, considering fault resistances $R_f = 0\ \Omega$ and $R_f = 10\ \Omega$, using 16 samples per cycle.

conventional algorithm to low sampling frequency when operating near the decision threshold.

3.3.3 Performance during external faults

The behaviour of the differential protection approaches in the case of an external fault located at the 50% of line L_2 is depicted in Figure 5, for three-phase faults. As observed in the test, both protection approaches perform adequately for single-phase-to-ground faults. However, for two-phase-to-ground and three-phase faults, the trip occurs at the conventional comparison-based line differential protection, thereby degrading the protection's performance. In the case of external faults, the differential protection is not expected to trip. Finally, the secure comparison-based line differential protection performs adequately in the case of the analysed external fault situations

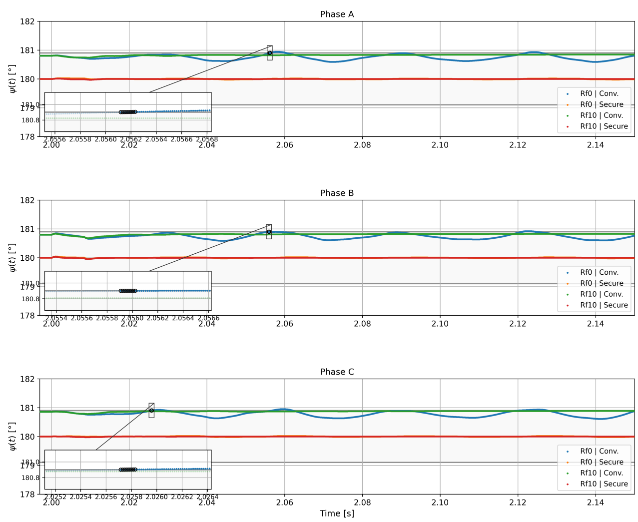

Figure 5: Protection performance for an external three-phase-to-ground fault located at 50 % of the line L_2, considering fault resistances $R_f = 0\ \Omega$ and $R_f = 10\ \Omega$, using 1024 samples per cycle.

4. Conclusion

Segregated phase comparison is a particular form of line differential protection and has been widely applied in conventional power systems due to its simplicity and its ability to discriminate faults based on angular information. However, its exclusive reliance on phase-angle differences makes it inherently sensitive to system disturbances, a condition exacerbated in scenarios with high penetration of inverter-based resources (IBRs), which were not considered in the original design of this protection scheme.

The results presented in this paper indicate that conventional segregated-phase comparison–based line differential protection may be limited under certain operating conditions involving IBRs. These limitations are observed under both pre-fault and fault conditions and become more pronounced as the number of phases involved in the fault increases, particularly for double-phase and three-phase-to-ground faults. Under these conditions, the angular difference between the currents measured at the local and remote terminals tends to increase. The secure segregated phase comparison-based line differential protection, incorporating compensation for the line capacitance effect, significantly reduces oscillations in the angular difference and ensures that, under pre-fault steady-state conditions, this difference remains practically constant. This behaviour helps to prevent undesired departures from the restraint region during normal load variations and minor system disturbances, thereby avoiding unnecessary line disconnections. In this context, proper tuning of the secure segregated phase comparison–based line differential protection improves angular trajectory stability, keeps it within the algorithm-defined restraint region, and prevents maloperation. Finally, although this protection strategy appears suitable, further studies are needed to assess the impact of variations in the magnitude of line capacitive compensation over extended periods of power-line operation.

Acknowledgment

The Vicerectoría de investigación, inovación y extensión funds this research through the project *Performance evaluation of non-pilot line protection relays in power systems with converter-interfaced generation*, code 6-25-3 at the Universidad Tecnológica de Pereira. The ICE^3 research group obtained this product.

References

[1] Saima Akhtar, Muhammad Adeel, Muhammad Iqbal, Abderrahmane Namoun, Ayesha Tufail, and Ki-Hyung Kim. Deep learning methods utilization in electric power systems. *Energy Reports*, 10:2138–2151, 2023.

[2] Maedeh Mahzarnia, Mohsen Parsa Moghaddam, Payam Teimourzadeh Baboli, and Pierluigi Siano. A review of the measures to enhance power systems resilience. *IEEE Systems Journal*, 14(3):4059–4070, 2020.

[3] V. A. Rosero-Morillo, F. Gonzalez-Longatt, J. M. Riquelme-Dominguez, and E. Orduña. Impact of inverter-based distributed generation integration on current seen by overcurrent relay: Cigre european mv network case. In *2023 IEEE Central America and Panama Convention (CONCAPAN XLI)*, pages 1–6, 2023.

[4] Hammad Khalid and Abdulfetah Shobole. Existing developments in adaptive smart grid protection: A review. *Electric Power Systems Research*, 191:106901, 2020.

[5] Jie Li, Jiahui Feng, Min Huang, Shuai Liu, and Guoqing Wang. Optimal protection coordination for directional overcurrent relays in radial distribution networks with inverter-based distributed energy resources. *International Journal of Electrical Power & Energy Systems*, 167:110622, 2025.

[6] Juan Cardenas. Line protection analysis on faults in networks with high penetration of inverter-based generation. recommendations for future improvements. In *19th International Conference on Developments in Power System Protection (DPSP Europe)*, pages 1–6, 2025.

[7] Soroush Sanati and Innocent Kamwa. A comprehensive review on differential protection schemes in ibr-dominated microgrids. *IEEE Access*, 12:170250–170271, 2024.

[8] Trupti P. Hinge and Sanjay S. Dambhare. Secure phase comparison schemes for transmission-line protection using synchrophasors. *IEEE Transactions on Power Delivery*, 30(4):2045–2054, 2015.

[9] Daniel M. Brasil, Carlos C. S. Silva, Kellen M. Silva, and Ricardo G. Bainy. On improving differential protection of lines interconnecting inverter-based resources. In *8th Workshop on Communication Networks and Power Systems (WCNPS)*, pages 1–6, 2023.

[10] Hugh Miller, John Burger, Norman Fischer, and Bogdan Kasztenny. Modern line current differential protection solutions. In *2010 IEEE Power and Energy Society General Meeting*, pages 1–9, 2010.

[11] Waldemar Rebizant, Armando Guzman, Stanley Zocholl, Zoran Djekic, and Mladen Kezunovic. Settingless protection: Feasibility study. In *19th International Conference on Developments in Power System Protection (DPSP Europe)*, pages 1–6, 2025.

[12] Saumendra Sarangi and Ashok Kumar Pradhan. Adaptive α-plane line differential protection. *IET Generation, Transmission & Distribution*, 11(10):2468–2477, 2017.

[13] B. Kasztenny, I. Voloh, and E.A. Udren. Rebirth of the phase comparison line protection principle. In *59th Annual Conference for Protective Relay Engineers*, page 60, 2006.

[14] H. Kang, A. Williams, and R. Squires. Phase comparison protection using adaptive carrier modulation. In *2005 IEEE Russia Power Tech*, pages 1–6, 2005.

[15] Trupti P. Hinge and Sanjay. S. Dambhare. Accurate phase comparison scheme with synchronised measurements. In *2015 IEEE Power Energy Society General Meeting*, pages 1–6, 2015.